Deep Learning-Based Real-Time Switching of Hybrid AC/DC Transmission Networks

Morteza Dabbaghjamanesh, *Senior Member, IEEE*, Amirhossein Moeini, *Member, IEEE*, Nikos D. Hatziargyriou, *Life Fellow, IEEE*, and Jie Zhang, *Senior Member, IEEE*

***Abstract*—In this article, a new deep learning-based framework is developed to perform real-time switching of hybrid AC/DC transmission grids under the effect of dynamic line rating (DLR) constraint. The proposed deep learning model is designed to learn the topological patterns of buses/lines according to operational states, e.g., power injections and line impedances, in order to obtain the optimal switchings of transmission power grids. As the load and power generation vary with time, the network switching depends on both the current and the previous status of the load and the generation units. Thus, a deep learning-based time series model that integrates the gated recurrent unit (GRU) and the long short-term memory (LSTM) models is developed, which takes advantage of LSTM's high accuracy and GRU's high computational efficiency. The developed learning-based network switching framework is tested on a modified hybrid AC/DC IEEE 39-bus system, a modified hybrid AC/DC 118-bus test system, and a modified hybrid AC/DC 300-bus test system. Results show that the learning-based switching model can achieve both high accuracy and computational efficiency, which is suitable for real-time transmission network switching.**

***Index Terms*—Hybrid AC/DC transmission grids, dynamic line rating, optimal switching, deep learning, long short-term memory, gated recurrent unit.**

NOMENCLATURE

Sets/Indices

RCS	Index of the remote control switch
Ω^D	Set of the CDOA control variables
Ω^H	Set of the CDOA population
i/Ω^{ADG}	Index/Set of the generation unit in the AC part
i/Ω^{DDG}	Index/Set of the generation unit in the DC part
k/Ω^S	Index/Set of switches
nm/Ω^{AL}	Index/Set of AC transmission lines
nm/Ω^{DL}	Index/Set of DC transmission lines
$l, n, m/\Omega^{AN}$	Index/Set of AC transmission node
$l, n, m/\Omega^{DN}$	Index/Set of DC transmission node
t/Ω^T	Index/Set of time
$\underline{(.)}/\overline{(.)}$	Indices of minimum and maximum values.

Parameters and Variables

A'	Transmission line projected area (m^2/Linear m)
C_i	Generation cost of ith unit
D_0	Transmission line diameter
$Hc/Zc, Zl$	Sun altitude/azimuth, transmission line azimuth
I_{it}	Binary status of ith unit.
$I^L_{nm,t}$	Distribution line current flow at time t
K_f	Thermal conductivity at air temperature
mCp	Transmission line heat capacity ($J/m-c$)
$N_{RCS,k}$	Number of switching actions of kth RCS
N_{loop}, N_{bus}	Network main loops, number of bus
N_{branch}	Branch number
P^G_{it}/Q^G_{it}	Active/reactive power of unit i at time t
P^D_t/Q^D_t	Active/reactive power demand
P^L_{nm}/Q^L_{nm}	Active/reactive power flow of line nm
Q_{se}	Radiated heat intensity of solar/sky
$q^c/q^r, q^s$	Convection/radiated heat loss, solar heat gain (W/m)
q^{cn}_{nmt}	Natural convection heat loss of transmission line nm at time t. (W/m)
$R(T_{avg})$	Transmission line AC resistance at temperature (T_{ave}) (Ω/m)
$R/X/\mathbb{Z}$	Resistance/reactance/impedance
SU/SD	Startup/shutdown cost
T	Transmission line temperature
T_{ave}	Transmission line Average temperature (c)
T_s, T_a	Transmission line surface and ambient air temperature (c)
V_{mt}	Voltage of bus m at time t
V_w	Velocity of the wind
$\Delta_{mn,t}$	Auxiliary variable
λ_{RCS}	Switching cost
θ_{nt}	Angle of bus n at time t
α	Solar absorptivity
ρ_f	Air density
μ_f	Transmission line dynamic viscosity of air temperature
β, θ	Angle between the transmission line and wind direction, Angle of sun's rays.

Manuscript received January 17, 2020; revised August 12, 2020 and October 17, 2020; accepted November 26, 2020. Date of publication December 2, 2020; date of current version April 21, 2021. Paper no. TSG-00081-2020. *(Corresponding author: Jie Zhang.)*

Morteza Dabbaghjamanesh and Jie Zhang are with the Department of Mechanical Engineering, The University of Texas at Dallas, Richardson, TX 75080 USA (e-mail: mortezadabba@utdallas.edu; jiezhang@utdallas.edu).

Amirhossein Moeini is with the Department of Electrical and Computer Engineering, Missouri University of Science and Technology, Rolla, MO 65409 USA (e-mail: amwfc@mst.edu).

Nikos D. Hatziargyriou is with the Electrical and Computer Engineering Department, National Technical University of Athens, Athens 157 73, Greece (e-mail: nh@power.ece.ntua.gr).

Color versions of one or more figures in this article are available at https://doi.org/10.1109/TSG.2020.3041853.

Digital Object Identifier 10.1109/TSG.2020.3041853

I. Introduction

TRANSMISSION networks can be classified into three main categories based on voltage types: AC, DC, and hybrid AC/DC. In AC transmission, all loads and distributed generators (DGs) are connected to the AC buses, while DC units are linked by AC/DC converters [1]. DC transmission lines utilize rectifiers to link the AC units to the electricity network, while DC loads are directly connected to the system [2]. In DC transmission grids, power losses can be decreased by reducing the power electronic-based interfaces. Furthermore, DC type power generation units, such as photovoltaic and batteries, can be connected to the DC network to supply DC loads, such as electric vehicle chargers and LED lights [3]. The benefits associated with both AC and DC transmission lines can be reflected in an interconnected configuration of transmission networks, known as hybrid AC/DC transmission grids. In such a configuration, loads and DG units are connected to their respective buses that can lead to a reduction in the number of power electronic-based interfaces. This implies higher efficiency, reliability, and lower operation and planning costs [4].

The optimal energy management of AC and DC transmission systems has been widely investigated. For instance, the optimal scheduling of the DC transmission grid has been solved in [5], by developing a dynamic piece-wise linear model. An iterative procedure has been proposed, in which the linear cuts are adjusted to approximate quadratic losses on each transmission line, iteratively. The day-ahead energy management by security-constrained unit commitment (SCUC), considering high voltage DC transmission line has been investigated in [6]. Optimal SCUC of DC transmission systems, considering transmission line outages and load shedding, has been formulated the problem as a mixed-integer linear programming (MILP) model [7]. A robust optimization approach was developed in [8], for optimal SCUC, considering the AC transmission network. The use of evolutionary algorithms to overcome the nonlinearity and non-convexity of the optimal power flow (OPF) in AC transmission systems was investigated in [9]. In [10] and [11], OPF for AC transmission systems was solved by linearizing the nonlinear constraints of the problem. Energy management of AC transmission systems considering dynamic line rating (DLR) effects was investigated in [12] by linearizing the AC power flow and DLR constraints. The effect of DLR on the conventional overhead transmission lines has been widely investigated in the literature. However, to the best of the authors' knowledge, the DLR constraint has not been investigated for hybrid AC/DC transmission grids. Since the operation of an AC/DC transmission grid is more complicated than that of a conventional AC transmission grid, due to power exchanging between the DC and AC parts, any changes in any parts can significantly influence the entire network. Thus, the influence of DLR on the AC power flow can affect both the AC and DC parts. To this end, considering the DLR constraint in the hybrid AC/DC transmission grid is more complicated and essential.

Energy management of AC and DC transmission systems has been widely investigated in the literature, hybrid AC/DC transmission grids, however, have not been well researched. This article investigates the optimal energy management of hybrid AC/DC transmission power grids, by considering DLR limitation of the overhead transmission lines. DLR can potentially affect the current flow in a conductor, especially in harsh and extreme weather conditions. To avoid any possible contingency or conductor overloading, as well as decreasing power losses, transmission switching of the system has been performed. Transmission switching is the process of changing the topology of the grid via prelocated switches. Transmission switching can bring significant benefits for the grid, e.g., enhanced reliability, load balance, voltage profile, as well as lower line losses [13], [14], [15]. The main focus of this article is real-time network switching of hybrid AC/DC transmission grids. In hybrid AC/DC grids, due to the high level of physical interconnectivity within the grid, a change in any part of the system (AC or DC) can affect the entire grid operation. Hence, compared to the conventional AC or DC grids, transmission switching plays a significant role in hybrid AC/DC grids energy management.

Hybrid AC/DC transmission switching is nonlinear and non-convex, due to the DLR and AC power flow nonlinear constraints. In the literature, heuristic and classic linearization algorithms have been used to solve this type of problem [3], [4]. It should be noted that solving the OPF problem using machine learning techniques has been widely investigated in the literature [16]. For instance, a supervised learning technique was used in [17] to solve real-time OPF problem. In [18], the OPF was solved using a machine learning technique, where the main objective is to predict the real power output of generators. The prediction of active OPF constraints was investigated in [19] and [20] to improve the computational efficiency of traditional physics-based solvers. However, in this research, the deep learning GRU-LSTM technique is adopted to not only solve the OPF problem, but also find out the optimal real-time transmission switching of the grids, which can be used under both normal and extreme conditions [16]. It should be noted that the power system size and complexity have been growing rapidly due to the increasing load demand and grid modernization. On the other hand, the loads and generation units are disproportionately increasing, which makes the grid more vulnerable to power outages. Furthermore, grid contingencies, natural disasters, and cyber/physical attacks are highly unpredictable and costly preventable, which require fast and reliable power flow analysis and transmission switching. To this end, conventional techniques may not be able to solve such a complex system with a reasonable computationally efficiency, especially in extreme conditions, where a fast and reliable power flow analysis and transmission switching are needed. To this end, in this article, unlike conventional methods, machine learning techniques are developed to provide a real-time transmission switching (in the order of microseconds). This can save the system from severe blackout and brownout.

In this article, for the first time, we propose a deep learning-based algorithm that aims to learn the topological patterns of buses/lines with their operating features, e.g., power injection and line impedance, in order to obtain the optimal switchings

of power grids. The inputs to the proposed deep learning model consist of the load and generation unit productions, while the outputs are the switching operations of the power network. It should be noted that the loads and power generation units vary with time, thus, the network switching depends on the current and previous states of the loads and generation units. A deep learning-based time series model is adopted, and more specifically, a deep learning of the gated recurrent unit (GRU) and the long short-term memory (LSTM) models is developed [21], [22]. The proposed deep learning of LSTM and GRU aims to take advantage of LSTM's high accuracy and GRU's high computational efficiency. The proposed deep learning-based algorithm provides twofold benefits: (i) high speed suitable for real-time implementation; and (ii) high accuracy. Thus, this technique is faster in comparison with conventional analytical and heuristic techniques that need to run the OPF. The proposed deep learning-based framework is tested on the modified hybrid AC/DC IEEE 39-bus, 118-bus, and 3008-bus test systems. Results have shown the effectiveness and merits of the proposed model. Also, in this article, the LSTM technique is utilized to forecast the hourly output power of photovoltaics (PVs). However, in this research the proposed deep learning GRU-LSTM technique is adopted to not only solve the OPF problem, but also find out the optimal real-time transmission switching of the grids, which can be used for both normal and extreme conditions. Overall, compared to existing studies in the literature, the main contributions of this article are summarized as follows.

- Apply the DLR constraint in the optimal operation of hybrid AC/DC transmission systems, along with other practical constraints. In hybrid AC/DC grids, due to the physical connectivity within the grid, any changes in the active or reactive power of the AC part (due to the DLR constraint) can affect the entire grid operation, including both AC and DC parts.
- Develop, for the first time, a deep learning model to find optimal real-time switchings of hybrid AC/DC transmission grids.

II. Dynamic Thermal Line Rating Limitation of the Overhead Transmission Lines

Dynamic line rating (DLR) is a practical limitation that can have a significant impact on the security and ampacity of the overhead transmission lines [23], [24]. Based on the IEEE std.738, the ampacity of the overhead transmission lines depends on the total heat losses and gains of the conductor in any time interval [25]. To this end, any changes in the conductor temperature in any time interval can affect the ampacity of the line as

$$I^{L}_{nmt} = \sqrt{\frac{q^{c}_{nmt} + q^{r}_{nmt} - q^{s}_{nmt} + mCp\left(\frac{dT_{ave}}{dt}\right)}{R(T_{ave})}} \tag{1}$$

The terms in Eq. (1) are heat losses and gains of the conductor, which can be calculated as follows.

A. Heat Losses

Heat losses of the conductor include convective and radiated heat losses [23].

1) Convective Heat Loss: The conductor convective heat loss is classified as natural convection and forced convection. For natural convection, the surrounding air cools the line (calm wind speed).

$$q^{cn}_{nmt} = (3.645)\rho_f^{0.5} D_0^{0.75}(T_s - T_a)^{1.25} \quad \forall t \in \Omega^{T}, \forall nm \in \Omega^{NA} \tag{2}$$

For forced convection, the surrounding air cools the line by a cylinder of moving air around the line. The forced convection can be taken into account for both low and high wind speeds as in (3) and (4), respectively.

$$q^{c1}_{nmt} = K_{angle}\Big[(1.01) + (1.35)N_{Re}^{0.52}K_f(T_s - T_a)\Big] \quad \forall t \in \Omega^{T}, \forall nm \in \Omega^{NA} \tag{3}$$

$$q^{c2}_{nmt} = K_{angle}(0.754){N_{Re}}^{0}.6K_f(T_s - T_a) \quad \forall t \in \Omega^{T}, \forall nm \in \Omega^{NA} \tag{4}$$

The Reynolds number N_{Re} and the wind direction K_{angle} are, respectively, calculated as

$$N_{Re} = \frac{(D_0)(\rho_f)(V_w)}{\mu_f} \tag{5}$$

$$K_{angle} = (1.194) - cos(\beta) + (0.194)cos(2\beta) + (0.3)sin(2\beta) \tag{6}$$

It should be noted that according to the IEEE std.738, the convection heat loss is the largest value among all of the possible scenarios (calm, low, and high wind speed). That means

$$q^{c}_{nmt} = max\Big(q^{cn}_{nmt}, q^{c1}_{nmt}, q^{c2}_{nmt}\Big) \tag{7}$$

2) Radiated Heat Loss: The conductor radiated heat loss can be calculated as

$$q^{r}_{nmt} = (17.8)(D_0)(\epsilon)\left(\left[\frac{T_s + 273}{100}^4\right] - \left[\frac{T_a - 273}{100}^4\right]\right) \quad \forall t \in \Omega^{T}, \forall nm \in \Omega^{NA} \tag{8}$$

where ϵ is the emissivity of the air.

B. Heat Gain

Heat gains of conductors include the solar and resistive heat gains [26].

1) Solar Heat Gain: The solar heat energy that can be gained by the line is known as the rate of solar heat gain, which can be taken into account as

$$q^{s}_{nmt} = (\alpha)(Q_{se})sin(\theta)A' \ \ \forall t \in \Omega^{T}, \forall nm \in \Omega^{NA} \tag{9}$$

where

$$\theta = arccos[cos(H_c) \times cos(Z_c - Z_l)]. \tag{10}$$

2) Resistive Heat Gain: Due to the resistive nature of lines, flowing the current to the transmission line can potentially heat up the line, which is known as resistive heat gain. This depends on the current and the resistance of the line. Based on the above explanations, the line average temperature can be obtained as:

$$\Delta T_{nmt} = \frac{\Delta t}{mCp}\Big[\big(I^L_{nmt}\big)^2 R_{nmt} + q^s_{nmt} - q^c_{nmt} - q^r_{nmt}\Big] \quad \forall t \in \Omega^T, \forall nm \in \Omega^{NA} \tag{11}$$

where Δt is the time step discretization of the heat balance equation. It should be noted that the DLR constraint can affect the active and reactive power of the AC power flow. However, in the hybrid AC/DC configuration, any changes in any subsystems (either AC or DC parts) can potentially affect the entire system. That means, changes in the AC power flow can affect the DC power flow and vis versa, since the entire network is physically connected.

III. Formulation for Switching of Hybrid AC/DC Transmission System

The objective and constraints of the optimal operation and switching of the hybrid AC/DC transmission grid can be defined as follows [27]–[29].

A. Objective Function

The objective is to minimize the total operation cost of the entire grid as in (12).

$$min \sum_{i\in\Omega^{DG}} \sum_{t\in\Omega^T} \Big[C_i P^G_{it} + SU_{it} + SD_{it}\Big] \tag{12}$$

where the first term of (12) is the operation cost, and the second term of (12) is the switching cost of the entire grid.

B. Constraints

The proposed optimization problem must satisfy constraints for both AC and DC parts, as follows:

1) AC Constraints: Equations (13)-(16) represent the power balance constraints on the AC part. Equations (13) and (14) ensure the active and reactive power balance at each AC bus, respectively, while (15) and (16) employ the Kirchhoff's Voltage Law (KVL) to the AC transmission lines, as shown in Fig. 1. The auxiliary variable $\Delta_{nm,t}$ in (15) can be zero, if line *mn* is switched ON at time *t*. Otherwise, it can be positive or negative, which is related to the voltage difference between the sending and receiving ends of the line *mn*. Active and reactive power of each generation unit should be within limits, as expressed in (17) and (18), while the voltage and angle of each bus should be constrained as (19) and (20), respectively. The number of transmission switchings per day should be lower than a maximum permissible number, as explained in (21). Finally, the DLR constraints are expressed in (22) and (23). These constraints ensure that the temperature of the lines at any time is lower than the maximum permissible temperature. It is worth noting that the DLR constraint depends on both active and reactive power. Hence, the DLR constraint has been applied to the AC part. However, since both AC and DC parts are connected and exchanging power in the hybrid AC/DC configuration, the DLR has indirect impact on the DC part as well.

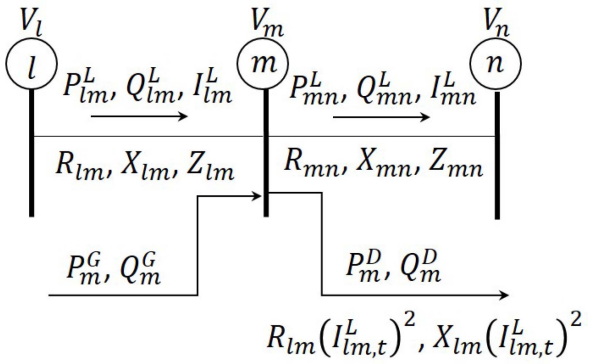

Fig. 1. Illustration of AC power balance.

$$\sum_{lm\in\Omega^L}\Big[P^L_{lm,t} - R_{lm}\big(I^L_{lm,t}\big)^2\Big] - \sum_{nm\in\Omega^L} P^L_{nm,t} + P^G_{imt} = P^D_{mt} \quad \forall i \in \Omega^{DG}, \forall t \in \Omega^T \tag{13}$$

$$\sum_{lm\in\Omega^L}\Big[Q^L_{lm,t} - X_{lm}\big(I^L_{lm,t}\big)^2\Big] - \sum_{nm\in\Omega^L} Q^L_{nm,t} + Q^G_{imt} = Q^D_{mt} \quad \forall i \in \Omega^{DG}, \forall t \in \Omega^T \tag{14}$$

$$(V_{mt})^2 - (V_{nt})^2 = 2\big(R_{nm}P^L_{nmt} + X_{nm}Q^L_{nmt}\big) - (\mathbb{Z}_{nm})^2\big(I^L_{nmt}\big)^2 + \Delta V_{nmt} \quad \forall nm \in \Omega^L, \forall n, m \in \Omega^N, \forall t \in \Omega^T \tag{15}$$

$$(V_{mt})^2\big(I^L_{nmt}\big)^2 = \big(P^L_{nmt}\big)^2 + \big(Q^L_{nmt}\big)^2 \quad \forall nm \in \Omega^L, \forall m \in \Omega^N, \forall t \in \Omega^T \tag{16}$$

$$\underline{P^G_i} I_{it} \le P^G_{it} \le \overline{P^G_i} I_{it} \quad \forall i \in \Omega^{DG}, \forall t \in \Omega^T \tag{17}$$

$$\underline{Q^G_i} I_{it} \le Q^G_{it} \le \overline{Q^G_i} I_{it} \quad \forall i \in \Omega^{DG}, \forall t \in \Omega^T \tag{18}$$

$$\underline{V_n} \le V_{nt} \le \overline{V_n} \quad \forall n \in \Omega^N, \forall t \in \Omega^T \tag{19}$$

$$-\pi \le \theta_{nt} \le \pi \quad \forall n \in \Omega^N, \forall t \in \Omega^T \tag{20}$$

$$N_{RCS,k,t} \le \overline{N_{RCS}} \quad \forall k \in \Omega^S, \forall t \in \Omega^T \tag{21}$$

$$P^L_{nmt}\big(T_{nm(t+1)} - T_{nmt}\big) = \Big[\big(I^L_{nmt}\big)^2 R_{nmt} + q^s_{nmt} - q^c_{nmt} - q^r_{nmt}\Big]; \forall t \in \Omega^T, \forall nm \in \Omega^{NA} \tag{22}$$

$$T_{nmt} \le T_{max} \quad \forall t \in \Omega^T, \forall nm \in \Omega^{NA}. \tag{23}$$

2) DC Constraints: Equations (24)-(32) present the DC network constraints. (24)-(28) represent generation unit constraints, like active powers of the generation units within limits by (24) and ramp up and down rates constrained as in (25) and (26), respectively. Accordingly, the minimum up and down time constraints of the generation units are presented in (27) and (28), respectively. DC network constraints are further set in (29-32), like power flow of DC transmission lines (29), nodal DC power balance (30), power flow limits of the DC transmission lines (31). Constraint (32) imposes the phase angle operational limits. Line flow limits are ensured by constraint (31), where $\underline{F_{nmt}} = -\overline{F_{nmt}}$, and similarly, $\underline{\theta_{mt}} = -\overline{\theta_{mt}}$.

Also, constraint (33) provides the reference angle at any time.

$$\underline{I_{it}P_i^G} \le P_{it}^G \le I_{it}\overline{P_i^G} \quad \forall t \in \Omega^T, \forall i \in \Omega^{DG} \tag{24}$$

$$P_{i,t}^G - P_{i,(t-1)}^G \le RU_i \quad \forall t \in \Omega^T, \forall i \in \Omega^{DG} \tag{25}$$

$$P_{i,(t-1)}^G - P_{i,t}^G \le RD_i \quad \forall t \in \Omega^T, \forall i \in \Omega^{DG} \tag{26}$$

$$T_{i,t}^{on} \ge UT_i\left(I_{it} - I_{i,(t-1)}\right) \quad \forall t \in \Omega^T, \forall i \in \Omega^{DG} \tag{27}$$

$$T_{i,t}^{off} \ge DT_i\left(I_{i(t-1)} - I_{i,t}\right) \quad \forall t \in \Omega^T, \forall i \in \Omega^{DG} \tag{28}$$

$$F_{nmt} = \frac{\theta_{mt} - \theta_{nt}}{X_{nm}} \quad \forall n, m \in \Omega^N \tag{29}$$

$$\sum F_{nmt} + \sum P_{it}^G + \sum P_{kt}^G = P_{mt}^D - L_{mt}^{sh} \quad \forall n, m \in \Omega^N, \forall i \in \Omega^{DG}, \forall k \in \Omega^{DGM} \tag{30}$$

$$\underline{F_{nmt}} \le F_{nmt} \le \overline{F_{nmt}} \quad \forall t \in \Omega^T, \forall nm \in \Omega^N \tag{31}$$

$$\underline{\theta_{mt}} \le \theta_{mt} \le \overline{\theta_{mt}} \quad \forall t \in \Omega^T, \forall m \in \Omega^N \tag{32}$$

$$\theta_{ref,t} = 0 \quad \forall t \in \Omega^T \tag{33}$$

Based on the mathematical formulations, the DLR is a thermal practical limitation that can affect both active and reactive power; that means it has an effect on the AC power flow. However, since the network is physically connected in the hybrid grids, a change in the AC part can affect the active power of the DC part.

To obtain the required training data, i.e., load and power generation, one-year load curves have been selected based on the real data from the California Independent System Operator (CAISO) [30] and the Electric Reliability Council of Texas [31] in year 2016, and used in the modified hybrid AC/DC IEEE 39-bus, 118-bus test, and 300-bust systems. It is worth noting that a heuristic technique, known as the collective decision optimization algorithm (CDOA), is adopted to solve the proposed nonlinear OPF problem. More information regarding the CDOA algorithm can be referred to Reference [23].

IV. Deep Learning Model for Transmission Network Switching

Different time-series learning-based techniques (e.g., recurrent neural networks, gated recurrent units, and long short-term memory, etc.) have been used in the literature for power system problems [17], [18]. However, using deep learning techniques for the switchings of the transmission systems has not been investigated in the literature. The main contribution of the proposed technique is to implement the switchings of the transmission system in real time by using deep learning techniques (i.e., gated recurrent units and long short-term memory). In conventional heuristic or mathematical techniques, the optimal switchings of transmission lines can be obtained after running the optimal power flow, which is a time-consuming process based on the number of buses and the complexity of the system. The proposed deep learning technique does not need to run the OPF in each hour to find the optimal switching transitions of the transmission system. Instead, the proposed technique finds the optimal switchings based on the load and generation units of the system, which leads to the real-time implementation of the OPF in transmission systems. Other machine learning techniques can also be used to obtain the switchings of the transmission systems. However, due to the nature of the transmission switchings (time-dependence) of power systems, in this article, advanced time series machine learning techniques (i.e., LSTM and GRU) are employed for the real-time transmission switchings.

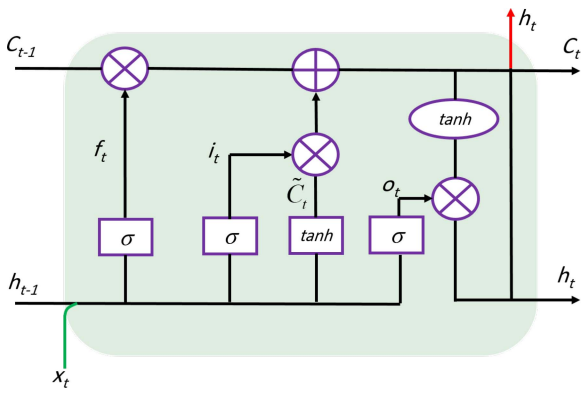

Fig. 2. The LSTM block diagram.

In this study, a new deep-learning technique is developed for obtaining the optimal switchings of the hybrid AC/DC transmission grids in real-time operation. Since the load and generation units vary with the time, network switching depends on both the current and previous status of the load and generation units. A deep learning-based time series model that integrates GRU and LSTM is developed, which takes advantage of LSTM′s high accuracy and GRU′s high computational efficiency.

A. Long Short-Term Memory Units

Long short-term memory (LSTM) was first introduced by Hochreiter and Schmidhuber in 1997 [22]. The main advantage of LSTM is that in long-term it avoids dependency on the data. Fig. 2 shows the block diagram of the LSTM unit. In this figure, there are three gates (input gate (i_t), forget gate (f_t) and output gate (o_t)) to control the flow of data from each unit. As shown in Fig. 2, the forget gate is obtained based on the following equation.

$$f_t = \sigma\left(W_f\left[h_{t-1}, x_t\right] + b_f\right) \tag{34}$$

where σ is a smooth and differentiable function like sigmoid. W_f and b_f are the constants for weight and bias of the forget gate, respectively. x_t is the current input data to the cell and h_{t-1} is the output data of the previous cell in (34). The input gate of the LSTM unit is controlled by the following equation.

$$i_t = \sigma\left(W_i\left[h_{t-1}, x_t\right] + b_i\right) \tag{35}$$

where W_i and b_i are the weight and the bias of the input gate, respectively. The new candidate value $\tilde{C}_t$ in Fig. 2 can be obtained by:

$$\tilde{C}_t = tanh\left(W_C\left[h_{t-1}, x_t\right] + b_C\right) \tag{36}$$

where W_C and b_C are the constants for the weight and the bias of the candidate layer, respectively. The future cell state C_t is obtained as shown below.

$$C_t = f_t \times C_{t-1} + i_t \times \tilde{C}_t \tag{37}$$

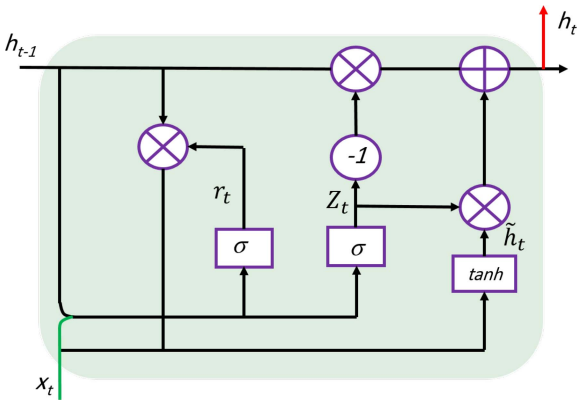

Fig. 3. The GRU block diagram.

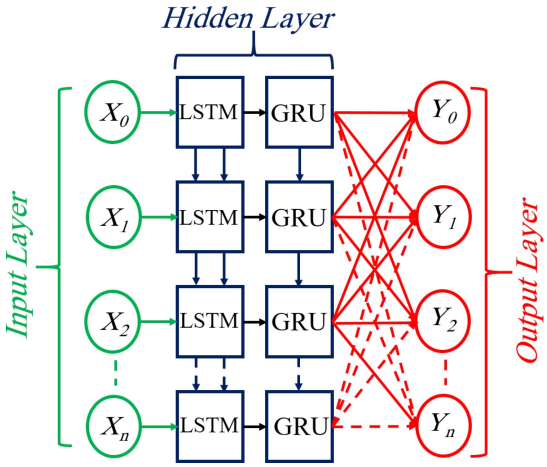

Fig. 4. Block diagram of the proposed deep learning GRU-LSTM.

Equation (37) determines the amount of data to be forgotten. Then the output gate of the LSTM unit is updated as shown below.

$$o_t = \sigma\left(W_o\left[h_{t-1}, x_t\right] + b_o\right) \tag{38}$$

where W_o and b_o are the constants for the weight and the bias of the output layer, respectively. The output of the cell h_t is obtained by the following equation as shown in Fig. 2.

$$h_t = o_t \times tanh(c_t) \tag{39}$$

B. Gated Recurrent Units

Chung *et al.* [21] proposed the gated recurrent unit (GRU) in 2014 to improve the performance of LSTM. The information flow in GRU is also controlled by different gates from input to output. The main block diagram of GRU is shown in Fig. 3.

$$h_t = (1 - z_t)h_{t-1} + z_t\tilde{h}_t \tag{40}$$

where z_t is an update gate that obtains the updates of each unit with its content or activation. This gate is updated by the following equation as shown in Fig. 3.

$$z_t = \sigma\left(U_z h_{t-1} + W_z x_t + b_z\right) \tag{41}$$

where σ is a differentiable and smooth activation function, U_z, W_z and b_z are the previous activation constant, input constant, and the bias of the update gate (z), respectively. The candidate activation in Fig. 3 and Eq. (40) can also be updated as:

$$\tilde{h}_t = tanh\left(U\left(r_t \bigodot h_{t-1}\right)Wx_t\right. \tag{42}$$

where $\bigodot$ is an element-wise multiplication. Moreover, r_t is the reset gate that is calculated as shown below.

$$r_t = \sigma\left(U_r h_{t-1} + W_r x_t + b_r\right) \tag{43}$$

In this article, the deep learning of GRU and LSTM is developed to solve the transmission network switching problem. As shown in Fig. 4, the hidden layers of the proposed model consists of both GRU and LSTM, in order to take advantage of both methods, which are high speed and accuracy.

It is worth noting that the inputs of the proposed deep-learning model are the load and generation unit powers, while the outputs of the proposed deep-learning model are the switching numbers of the hybrid AC/DC transmission network.

TABLE I
THE HYPER-PARAMETERS OF THE PROPOSED TECHNIQUE

Parameters	Values
Learning rate	0.001
β_1	0.9
β_2	0.999
E	10^{-7}

V. SIMULATION RESULTS

In this section, results for optimal switchings of modified hybrid AC/DC IEEE 39-bus, IEEE 118-bus, IEEE 300-bus are provided to show the effectiveness and merits of the proposed deep learning-based transmission network switching framework.

A pre-processing technique (scaling) is used for the learning techniques to normalize the input and output data between 0 and 1. Furthermore, the computer used for model training has a CPU with Intel Core i5-8250U and 1.6GHz, and 8GB RAM. The information of model training is shown in Table III, including the test system, machine learning technique, training time (with 1,500 epochs and a batch size of 300), and validation accuracy. The hyper-parameters of the ADAM optimizer have been summarized in Table I. It should be noted that the default values in the Keras library [32] are adopted for the ADAM optimizer. The ANN and RNN techniques are selected as benchmark models to compare with the proposed deep learning techniques, and comparison results as summarized in Table II. In the proposed technique, two hidden layers are used for all learning techniques in Table II. In each hidden layer, 100 nodes are used. Furthermore, the ADAM optimizer technique is used to train all deep learning techniques in Table II. Also, the proposed technique uses the optimal power flow to obtain the switching status for model training. The information of model training is shown in Table II, including the test system, machine learning technique, training time (with 1,500 epochs and a batch size of 300), and validation accuracy. Furthermore, the ratio of validation/training data is 1/4. In this table, the training data of each technique for different IEEE standard systems are shown. The accuracy of the training of the three deep learning techniques for the three IEEE standards are compared in Table II.

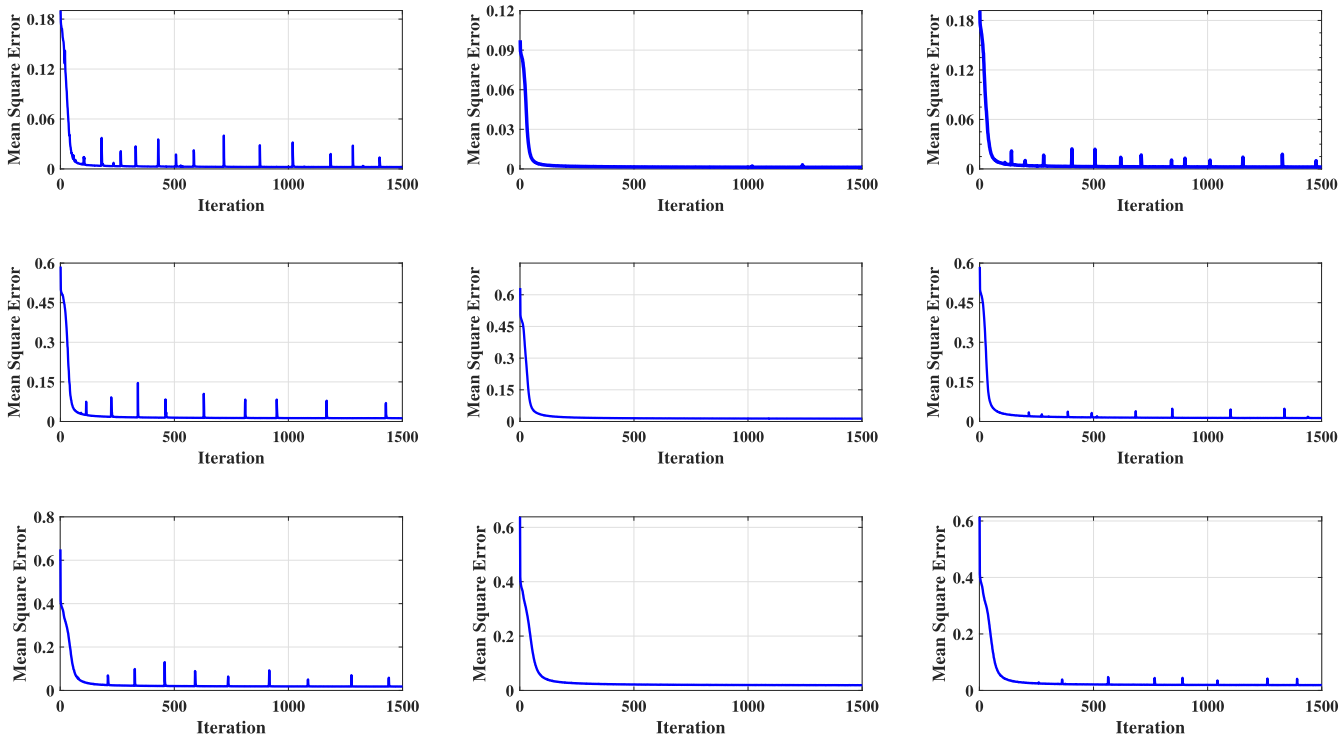

Fig. 5. MSE of the deep learning technique for test systems. (a) LSTM with 39-bus, (b) GRU with 39-bus, (c) the proposed deep learning technique with 39-bus, (d) LSTM with 118-bus, (e) GRU with 118-bus, (f) the proposed deep learning technique with 118-bus (g) LSTM with 300-bus, (h) GRU with 300-bus, (i) the proposed deep learning technique with 300-bus.

Furthermore, the mean square errors (MSE) of the training of the three deep learning techniques also are shown in Fig. 5. In the proposed technique, a round function is used to find integer numbers for the switchings of the transmission system in the proposed deep learning technique.

A. Modified Hybrid IEEE 39-Bus Test System

In this subsection, the proposed deep learning-based transmission network switching technique is utilized to solve the modified IEEE 39-bus test system. Fig. 6 shows a single line diagram of the modified IEEE 39-bus test system, which is equipped with two bidirectional AC/DC converters (i.e., main and backup converters) that coordinate the power flow between the AC and DC parts. The system includes one fuel cell (FC), two microturbines (MTs), and five tie switches. It should be noted that the characteristics of the transmission tie switching lines are same as the closes line, based on IEEE networks standards in MATPOWER [33]. It also contains one photovoltaic (PV) and two WTs as non-dispatchable generation units.

Figs. 7 and 8 depict the hourly forecasted values of the wind and solar power, respectively. It should be noted that PV and WTs power is forecasted by the LSTM model, which has been widely used for renewable power forecasting due to its high accuracy [34], [35]. Table II lists the root mean square error (RMSE), mean square error (MSE), and mean absolute error (MAE) of the LSTM forecasts.

Fig. 9 shows the optimal switchings of the hybrid network, obtained by the conventional optimization-based technique (CT) and the proposed deep learning-based technique (PT). It is seen that the optimal switching obtained by the proposed technique is similar to those of the conventional one with a very small difference. Specifically, in the first hour, switching numbers S1 and S4 are different, while in the last hour there is no difference. The optimal output power of the FC and MTs for both CT and PT is shown in Fig. 10. It is seen that there exists a difference between the two techniques. For instance, at hour 12, the FC is committed with its maximum capacity in the conventional method, while the FC unit is OFF

TABLE II
TIME DURATION OF THE TRAINING OF THE PROPOSED TECHNIQUE FOR TWO SCENARIOS OF SIMULATIONS

Case	Learning Technique	Number of data data (hour)	Training duration (hour)	MSE of validation
39-bus	ANN	349 days	0:3	0.0315
39-bus	RNN	349 days	0:51	0.0027
39-bus	LSTM	349 days	1:50	0.0023
39-bus	GRU	349 days	1:41	0.0025
39-bus	Proposed model	349 days	1:48	0.0023
118-bus	ANN	299 days	0:2	0.34
118-bus	RNN	299 days	0:49	0.016
118-bus	LSTM	299 days	1:44	0.0125
118-bus	GRU	299 days	1:31	0.0137
118-bus	Proposed model	299 days	1:36	0.0132
300-bus	LSTM	297 days	1:53	0.0179
300-bus	GRU	297 days	1:25	0.01917
300-bus	Proposed model	297 days	1:28	0.0187

TABLE III
RMSE, MSE, AND MAE OF LSTM FORECASTING MODELS

Generation Unit	RMSE (kW)	MSE (kW^2)	MAE (kW)
Wind turbine	0.0490	0.0024	0.0290
Photovoltaic	0.0592	0.0035	0.0332

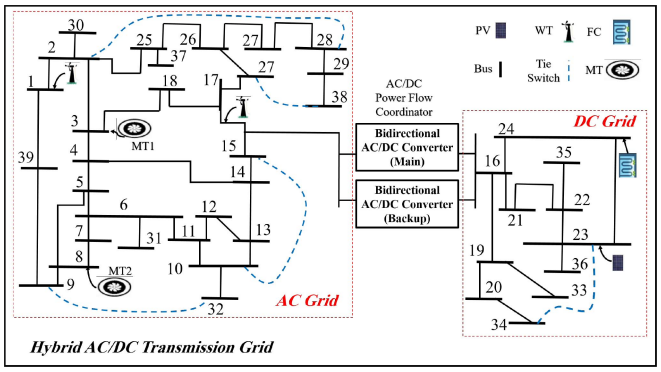

Fig. 6. Modified hybrid AC/DC IEEE 39-bus test system.

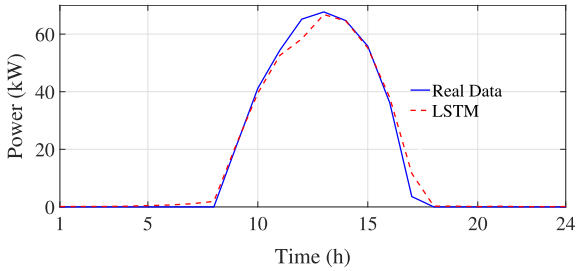

Fig. 7. Hourly solar power forecasts.

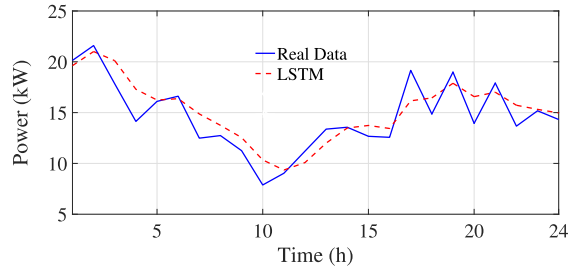

Fig. 8. Hourly wind power forecasts.

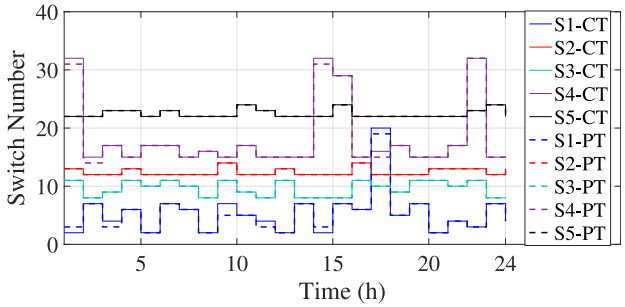

Fig. 9. IEEE 39-bus optimal switchings from both the conventional optimization-based technique (CT) and the proposed deep learning-based technique (PT).

in the deep-learning based method. Despite some differences in the output power of the generation units, the total operation cost of the conventional and proposed techniques is very similar, \$130,060.6 and \$131,182.6, respectively. It is worth noting that the learning-based cost is obtained by applying the learning-based switching result into the conventional method and run the OPF.

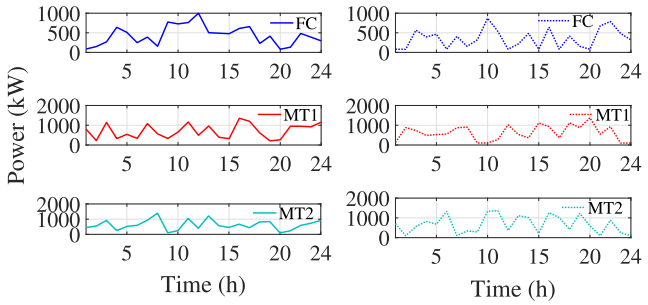

Fig. 10. IEEE 39-bus output power of the FC, MT1, and MT2 from both CT (left-hand side) and PT (right-hand side).

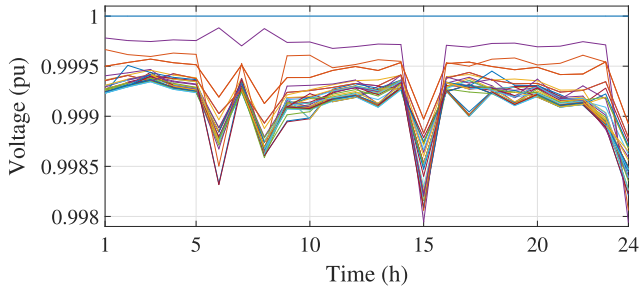

Fig. 11. IEEE 39-bus voltages by using the proposed deep learning-based technique.

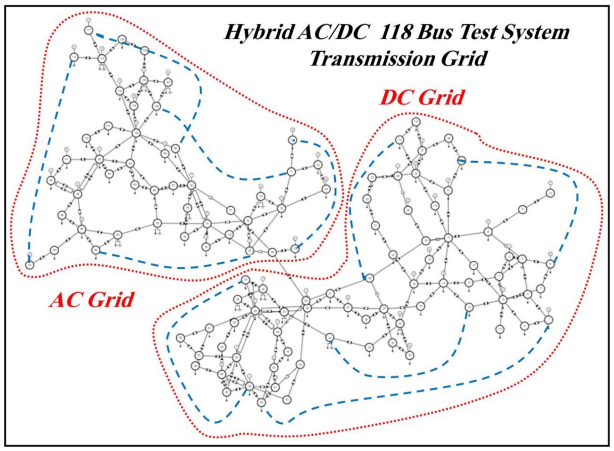

Fig. 12. Modified hybrid IEEE 118-bus test system.

Fig. 11 depicts the per unit (pu) voltage magnitudes at all buses for the entire horizon, obtained by the proposed learning-based technique. It is shown that all voltages are within limits, which proves the good performance of the deep learning-based transmission network switching.

B. Modified Hybrid IEEE 118-Bus Test System

The proposed method is also tested on a modified hybrid IEEE 118-bus test system. Fig. 12 shows the single line diagram of the test network, which contains three FCs and five PVs in the DC part, and three WTs and five MTs in the AC part. The PVs and WTs have the same production patterns, as in Figs. 7 and 8. Similarly, two bidirectional AC/DC converters (i.e., main and backup) are considered to coordinate the power flow between AC and DC parts. Similar to the previous case,

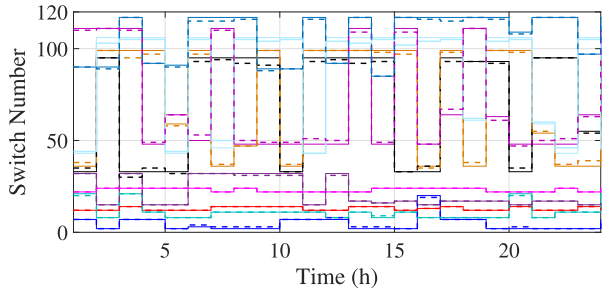

Fig. 13. IEEE 118-bus optimal switchings from both the conventional and the deep learning techniques.

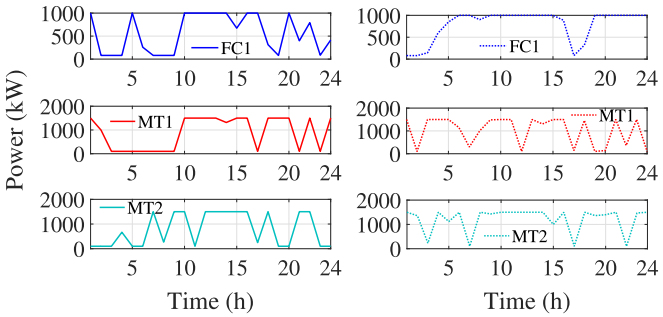

Fig. 14. IEEE 118-bus output power of the FC1, MT1, and MT2 for both the conventional technique (left-hand side) and the deep learning technique (right-hand side).

the AC part is under the effect of the DLR constraint to have a more realistic model. The 118-bus network includes ten tie switches (five in each part), which are initially open. It should be noted that IEEE 39 bus test system transmission lines have the same ambient conditions and temperature. However, at the transmission level, different weather conditions are considered for the IEEE 118 bus test system to provide a more realistic model, which is taken from [24].

Fig. 13 depicts the optimal switchings obtained by conventional and proposed techniques. As shown, the optimal switchings of the proposed deep-learning method are very close to those of the conventional technique. Although these small changes can affect the output power of some DGs, the total operation cost of the proposed technique is very similar to that of the conventional technique.

Fig. 14 shows the output power of MT1, MT2, and FC1 obtained by each technique. The total operation costs are \$44,458.6 and \$44,778.7, respectively. Fig. 15 shows the bus voltage magnitudes for the entire horizon. Same as in the IEEE 39-bus case, the bus voltages are within limits, which also validates the high performance of the proposed technique for large-scale grids.

Table IV shows the convergence speed of the conventional and the proposed deep learning-based techniques for the test systems, which shows the high computational efficiency of the proposed learning-based technique (in order of microseconds).

C. Modified Hybrid IEEE 300-Bus Test System

The proposed technique is also tested for the IEEE 300-bus system as shown in Fig. 16. The network includes 69 generators, 60 LTCs, 304 transmission lines, and 195 loads. For

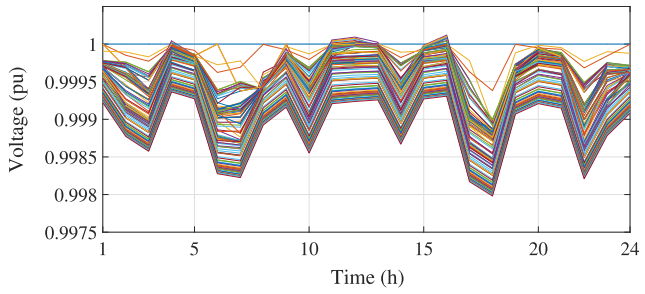

Fig. 15. IEEE 118-bus voltages by using the proposed deep learning-based technique.

TABLE IV
CONVERGENCE SPEED OF BOTH CONVENTIONAL OPTIMIZATION-BASED AND DEEP LEARNING-BASED METHODS

Technique	Test System	Convergence Speed
Conventional optimization-based	39-bus	17.9 (s)
Conventional optimization-based	118-bus	79.2 (s)
Conventional optimization-based	300-bus	285.2 (s)
Deep learning-based	39-bus	1.7 (μs)
Deep learning-based	118-bus	3.4 (μs)
Deep learning-based	300-bus	8.9 (μs)

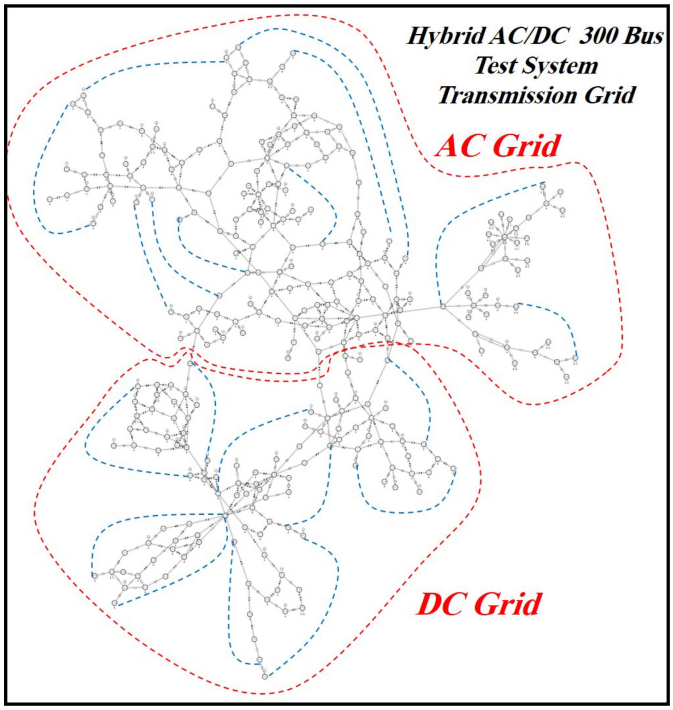

Fig. 16. Modified hybrid IEEE 300-bus test system.

the IEEE 300-bus system, 20 tie switches are used in this article to switch the hybrid transmission grid. Figs. 5(g), (h), and (i) show the MSE of the LSTM, GRU, and proposed deep learning techniques. Fig. 17 shows the optimal switching of the hybrid AC/DC IEEE 300-bus test system for both the conventional and learning-based techniques. Similar to the previous cases, there exist small difference between the optimal switchings of the conventional and proposed techniques. However, the total operation costs of these techniques are close (see Table V). Fig. 18 depicts the per unit (pu) voltage magnitudes

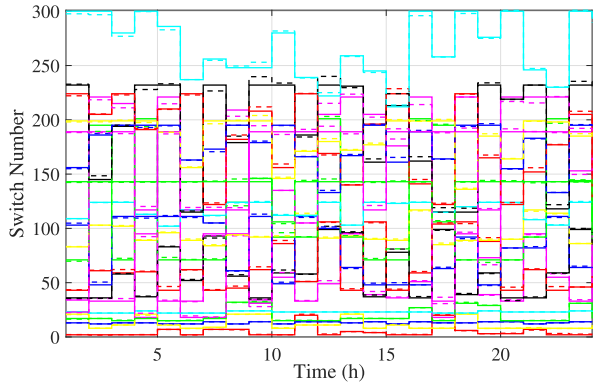

Fig. 17. IEEE 300-bus optimal switchings from both the conventional (solid lines) and the deep learning techniques (dashed lines).

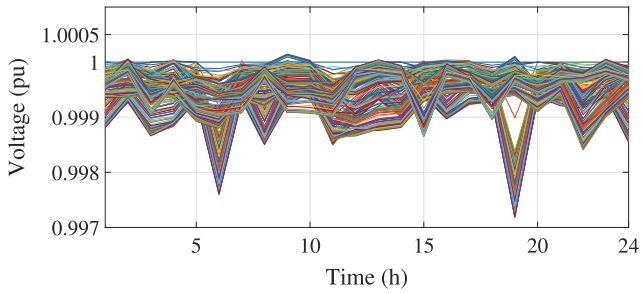

Fig. 18. IEEE 300-bus voltages by using the proposed deep learning-based technique.

at all buses for the entire horizon, obtained by the proposed learning-based technique. It is shown that all voltages are within limits, which proves the high performance of the deep learning-based method for large-scale transmission network switching.

Table V compares the total operation costs of the test networks with and without the DLR constraint. It is observed that considering DLR as an independent constraint impacts the operation costs of the proposed problem. For instance, by considering DLR, the total operation costs of the IEEE 39 and IEEE 118 bus test systems are increased by approximately 3% and 5%, respectively. This is the cost that should be paid to operate the transmission grids in a more realistic environment, thereby enhancing the security and reliability of the network.

In this article, simulation results of the switchings of the transmission systems during steady state conditions are shown. The transient and dynamic conditions of the transmission systems are also important, which will be studied in future work. Also, it should be noted that the AC/DC converter control plays a significant role in the energy management of hybrid AC/DC grids. However, in this study, we assume that the converter controller has been tuned perfectly [3], and only the power limits constraints are considered. The influence of the bidirectional AC/DC converter control on the performance of the hybrid AC/DC transmission system will be investigated in potential future work. Moreover, it is worth noting that the main focus of this research is transmission switching, neglecting the distribution system

TABLE V
TOTAL OPERATION COST

Test System	Operation Cost ($)			
	Conventional Technique		Proposed Technique	
	Without DLR	With DLR	Without DLR	With DLR
IEEE 39	127,459.3	130,060.6	128,102.02	131,182.6
IEEE 118	42,235.7	44,458.6	42,315.8	44,778.7
IEEE 300	117,143.6	125,853.2	117,107.7	125,983.9

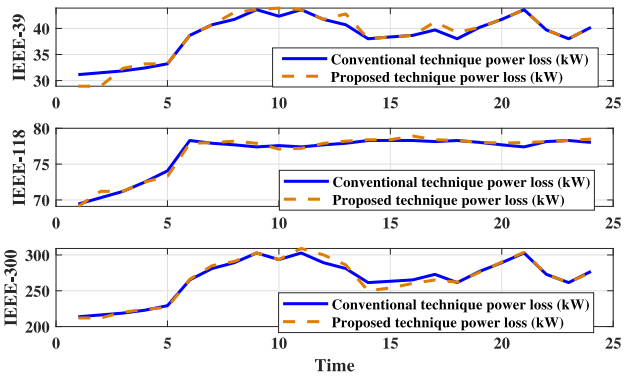

Fig. 19. Power losses of both conventional and proposed techniques.

integration [24], [36]. Potential future work will explore the integration of transmission switching and distribution reconfiguration.

Fig. 19 depicts the hourly power losses of IEEE 39, 118 and 300 bus test systems with both the conventional and proposed techniques. Although there exist differences in both the power output of generation units and transmission switching, the power losses of both the conventional and proposed techniques are close, which proves the effectiveness and merit of the proposed technique.

VI. CONCLUSION

This article developed an offline learning-based transmission network switching technique by using a deep learning model of long short-term memory and gated recurrent unit. Optimal switchings of the transmission hybrid AC/DC power grids are obtained by the deep learning-based method, considering the overhead dynamic line rating constraint. The proposed technique was applied to a medium (hybrid IEEE 39-bus) scale power grid, as well as two large scale power grids (hybrid IEEE 118-bus and hybrid IEEE 300-bus). Compared to conventional optimization-based techniques, the deep-learning technique for network switching has two advantages: (i) it allows real-time application (i.e., high computational efficiency) of the proposed technique along with more flexibility and extendibility, and (ii) it provides highly accurate results comparable to conventional methods. Although the optimal switchings and the output power of DGs obtained by the two methods are not exactly matched, the total operation cost of the proposed learning-based method is very close to that of the conventional optimization-based technique (i.e., less than 1% difference).

REFERENCES

[1] M. Dabbaghjamanesh, S. Mehraeen, A. Kavousi-Fard, and F. Ferdowsi, "A new efficient stochastic energy management technique for interconnected AC microgrids," in *Proc. IEEE Power Energy Soc. Gen. Meeting (PESGM)*, 2018, pp. 1–5.

[2] M. A. Elizondo *et al.*, "Interarea oscillation damping control using high-voltage DC transmission: A survey," *IEEE Trans. Power Syst.*, vol. 33, no. 6, pp. 6915–6923, Nov. 2018.

[3] B. Papari, C. S. Edrington, I. Bhattacharya, and G. Radman, "Effective energy management of hybrid AC–DC microgrids with storage devices," *IEEE Trans. Smart Grid*, vol. 10, no. 1, pp. 193–203, Jan. 2019.

[4] M. Dabbaghjamanesh, A. Kavousifard, S. Mehraeen, J. Zhang, and Z. Y. Dong, "Sensitivity analysis of renewable energy integration on stochastic energy management of automated reconfigurable hybrid AC–DC microgrid considering DLR security constraint," *IEEE Trans. Ind. Informat.*, vol. 16, no. 1, pp. 120–131, Jan. 2020.

[5] T. N. Dos Santos and A. L. Diniz, "A dynamic piecewise linear model for DC transmission losses in optimal scheduling problems," *IEEE Trans. Power Syst.*, vol. 26, no. 2, pp. 508–519, May 2011.

[6] A. Lotfjou, M. Shahidehpour, and Y. Fu, "Hourly scheduling of DC transmission lines in SCUC with voltage source converters," *IEEE Trans. Power Del.*, vol. 26, no. 2, pp. 650–660, Apr. 2011.

[7] J. Liu, M. Kazemi, A. Motamedi, H. Zareipour, and J. Rippon, "Security-constrained optimal scheduling of transmission outages with load curtailment," *IEEE Trans. Power Syst.*, vol. 33, no. 1, pp. 921–931, Jan. 2018.

[8] Y. K. Renani, M. Ehsan, and M. Shahidehpour, "Day-ahead self-scheduling of a transmission-constrained GenCo with variable generation units using the incomplete market information," *IEEE Trans. Sustain. Energy*, vol. 8, no. 3, pp. 1260–1268, Jul. 2017.

[9] W. Yan, F. Liu, C. Chung, and K. Wong, "A hybrid genetic algorithm-interior point method for optimal reactive power flow," *IEEE Trans. Power Syst.*, vol. 21, no. 3, pp. 1163–1169, Aug. 2006.

[10] C. Liu, M. Shahidehpour, Y. Fu, and Z. Li, "Security-constrained unit commitment with natural gas transmission constraints," *IEEE Trans. Power Syst.*, vol. 24, no. 3, pp. 1523–1536, Aug. 2009.

[11] K. Meng, W. Zhang, J. Qiu, Y. Zheng, and Z. Y. Dong, "Offshore transmission network planning for wind integration considering AC and DC transmission options," *IEEE Trans. Power Syst.*, vol. 34, no. 6, pp. 4258–4268, Nov. 2019.

[12] J. Zhan, W. Liu, and C. Chung, "Stochastic transmission expansion planning considering uncertain dynamic thermal rating of overhead lines," *IEEE Trans. Power Syst.*, vol. 34, no. 1, pp. 432–443, Jan. 2019.

[13] A. Kavousi-Fard, T. Niknam, H. Taherpoor, and A. Abbasi, "Multi-objective probabilistic reconfiguration considering uncertainty and multi-level load model," *IET Sci. Meas. Technol.*, vol. 9, no. 1, pp. 44–55, Jan. 2015.

[14] M. Kashem, V. Ganapathy, and G. Jasmon, "Network reconfiguration for load balancing in distribution networks," *IEE Proc. Gener. Transm. Distrib.*, vol. 146, no. 6, pp. 563–567, 1999.

[15] A. Kavousi-Fard and T. Niknam, "Optimal distribution feeder reconfiguration for reliability improvement considering uncertainty," *IEEE Trans. Power Del.*, vol. 29, no. 3, pp. 1344–1353, Jun. 2014.

[16] B. Donnot, "Deep learning methods for predicting flows in power grids: Novel architectures and algorithms," Ph.D. dissertation, Sciences et Technologies de L'information et de la Communication (STIC), Université Paris Saclay (COmUE), Gif-sur-Yvette, France, 2019.

[17] R. Canyasse, G. Dalal, and S. Mannor, "Supervised learning for optimal power flow as a real-time proxy," in *Proc. IEEE Power Energy Soc. Innov. Smart Grid Technol. Conf. (ISGT)*, 2017, pp. 1–5.

[18] X. Lei, Z. Yang, J. Yu, J. Zhao, Q. Gao, and H. Yu, "Data-driven optimal power flow: A physics-informed machine learning approach," *IEEE Trans. Power Syst.*, early access, Jun. 12, 2020, doi: 10.1109/TPWRS.2020.3001919.

[19] A. Robson, M. Jamei, C. Ududec, and L. Mones, "Learning an optimally reduced formulation of OPF through meta-optimization," 2019. [Online]. Available: arXiv:1911.06784.

[20] Y. Ng, S. Misra, L. A. Roald, and S. Backhaus, "Statistical learning for DC optimal power flow," in *Proc. Power Syst. Comput. Conf. (PSCC)*, 2018, pp. 1–7.

[21] J. Chung, C. Gulcehre, K. Cho, and Y. Bengio, "Empirical evaluation of gated recurrent neural networks on sequence modeling," 2014. [Online]. Available: arXiv:1412.3555.

[22] S. Hochreiter and J. Schmidhuber, "Long short-term memory," *Neural Comput.*, vol. 9, no. 8, pp. 1735–1780, 1997.

[23] M. Dabbaghjamanesh, A. Kavousi-Fard, and S. Mehraeen, "Effective scheduling of reconfigurable microgrids with dynamic thermal line rating," *IEEE Trans. Ind. Electron.*, vol. 66, no. 2, pp. 1552–1564, Feb. 2019.

[24] M. Nick, O. Alizadeh-Mousavi, R. Cherkaoui, and M. Paolone, "Security constrained unit commitment with dynamic thermal line rating," *IEEE Trans. Power Syst.*, vol. 31, no. 3, pp. 2014–2025, May 2016.

[25] *IEEE Standard for Calculating the Current-Temperature Relationship of Bare Overhead Conductors*, IEEE Standard 738-2012, Sep. 2012.

[26] M. Dabbaghjamanesh, A. Kavousi-Fard, and Z. Dong, "A novel distributed cloud-fog based framework for energy management of networked microgrids," *IEEE Trans. Power Syst.*, vol. 35, no. 4, pp. 2847–2862, Jul. 2020.

[27] C. Lin, W. Wu, and M. Shahidehpour, "Decentralized AC optimal power flow for integrated transmission and distribution grids," *IEEE Trans. Smart Grid*, vol. 11, no. 3, pp. 2531–2540, May 2020.

[28] G. Liang, S. R. Weller, J. Zhao, F. Luo, and Z. Y. Dong, "A framework for cyber-topology attacks: Line-switching and new attack scenarios," *IEEE Trans. Smart Grid*, vol. 10, no. 2, pp. 1704–1712, Mar. 2019.

[29] G. J. Kish, "On the emerging class of non-isolated modular multilevel DC–DC converters for DC and hybrid AC–DC systems," *IEEE Trans. Smart Grid*, vol. 10, no. 2, pp. 1762–1771, Mar. 2019.

[30] *California Independent System Operator*. Accessed: Aug. 2019. [Online]. Available: http://oasis.caiso.com/mrioasis/logon.do

[31] *Electric Reliability Council of Texas*. Accessed: Aug. 2019. [Online]. Available: http://www.ercot.com/gridinfo/load

[32] F. Chollet *et al.* (2015). Accessed: Aug. 2019. *Keras*. [Online]. Available: https://keras.io

[33] *Matpower Free, Open-Source Tools for Electric Power System Simulation and Optimization*. Accessed: Aug. 2019. [Online]. Available: https://matpower.org/

[34] X. Qing and Y. Niu, "Hourly day-ahead solar irradiance prediction using weather forecasts by LSTM," *Energy*, vol. 148, pp. 461–468, Apr. 2018.

[35] H. Liu, X. Mi, and Y. Li, "Smart multi-step deep learning model for wind speed forecasting based on variational mode decomposition, singular spectrum analysis, LSTM network and ELM," *Energy Convers. Manag.*, vol. 159, pp. 54–64, Mar. 2018.

[36] E. B. Fisher, R. P. O'Neill, and M. C. Ferris, "Optimal transmission switching," *IEEE Trans. Power Syst.*, vol. 23, no. 3, pp. 1346–1355, Aug. 2008.

Morteza Dabbaghjamanesh (Senior Member, IEEE) received the M.Sc. degree in electrical engineering from Northern Illinois University, DeKalb, IL, USA, in 2014, and the Ph.D. degree in electrical and computer engineering form Louisiana State University, Baton Rouge, LA, USA, in 2019. He is currently a Research Associate with the Design and Optimization of Energy Systems Laboratory, University of Texas at Dallas, Richardson, TX, USA. His current research interests include power system operation and planning, reliability, resiliency, renewable energy sources, cybersecurity analysis, machine/deep learning, smart grids, and microgrids.

Amirhossein Moeini (Member, IEEE) received the Ph.D. degree in electrical engineering from the University of Florida, Gainesville, FL, USA, in 2019. He is currently a Postdoctoral Research Fellow with the Department of Electrical and Computer Engineering, Missouri University of Science and Technology. He published more than 25 journal and conference papers and holds three USA patents. His current research interests include power electronics, multilevel converters, deep/machine learning, battery management, and EV charging stations.

Nikos D. Hatziargyriou (Life Fellow, IEEE) is a Professor with the Power Systems, National Technical University of Athens. He has participated in more than 60 RDD projects funded by the EU Commission, electric utilities and manufacturers for both fundamental research and practical applications. He has authored the book *Microgrids: Architectures and Control* and more than 250 journal publications and 500 conference proceedings papers. He has over ten year industrial experience as the Chairman and as the CEO of the Hellenic Distribution Network Operator and as an Executive Vice-Chair of the Public Power Corporation. He was the Chair and currently the Vice-Chair of the EU Technology and Innovation Platform on Smart Networks for Energy Transition representing E.DSO. He is the past Chair of the Power System Dynamic Performance Committee and currently the Editor-in-Chief of the IEEE TRANSACTIONS ON POWER SYSTEMS. He is included in the 2016, 2017, and 2019 Thomson Reuters lists of the top 1% most cited researchers. He is an Honorary Member of CIGRE and the past Chair of CIGRE SC C6 "Distribution Systems and Distributed Generation."

Jie Zhang (Senior Member, IEEE) received the B.S. and M.S. degrees in mechanical engineering from the Huazhong University of Science and Technology, Wuhan, China, in 2006 and 2008, respectively, and the Ph.D. degree in mechanical engineering from Rensselaer Polytechnic Institute, Troy, NY, USA, in 2012. He is currently an Assistant Professor with the Department of Mechanical Engineering, the University of Texas at Dallas. His research interests include multidisciplinary design optimization, complex engineered systems, big data analytics, wind and solar forecasting, renewable integration, and energy systems modeling and simulation.